

Structural Diversity in Zinc Phosphates and Phosphinates: Observation of a Lattice Water Dimer Sandwiched Between Phosphoryl Oxygen Atoms

Ramasamy Pothiraja,^[a] Swaminathan Shanmugan,^[a] Mrinalini G. Walawalkar,^{*,[a]} Munirathinam Nethaji,^[b] Ray J. Butcher,^[c] and Ramaswamy Murugavel^{*,[a]}

Keywords: Molecular phosphates / Zinc phosphinates / Polymers / Water clusters / X-ray diffraction

Reactions of zinc acetate dihydrate with organic phosphates $[(RO)_2P(O)(OH)]$ ($R = tBu, Ph$) and phosphinic acids $[PhR'P(O)(OH)]$ ($R' = Ph, H$) have been investigated in the presence of 1,10-phenanthroline (phen). While the use of *tert*-butyl phosphate (dtbp-H) results in the formation of $[Zn(phen)_2(dtbp)(OH_2)][dtbp](MeOH)(MeCOOH)(H_2O)_3$ (**1**), the change of phosphorus source to diphenylphosphate (dpp-H) yields an interesting phosphate-bridged dinuclear complex $[Zn(phen)(dpp)]_2[\mu_2-dpp]_2$ (**2**). Mononuclear complexes $[Zn(phen)_2(dppi)_2](H_2O)_2$ (**3**) and $[Zn(phen)_2(ppi)_2](H_2O)$ (**4**) have been obtained from similar reactions by the use of diphenylphosphinic acid (dppi-H) and phenylphosphinic acid (ppi-H), respectively. The high steric bulk of the dtbp ligand results in the formation of the cationic complex **1**, where only one of the dtbp ligands is directly coordinated to the metal atom, leaving the second dtbp molecule as the counter anion. The inorganic core of dinuclear zinc phosphate **2** resembles the single four-ring (S4R) secondary build-

ing unit of framework zinc phosphates. Compounds **3** and **4** are neutral monomeric hexacoordinate complexes with two chelating 1,10-phen ligands and two monodentate phosphinate ligands. The two lattice water molecules in **3** form an interesting water dimer $(H_2O)_2$. These water dimers link the mononuclear zinc complexes in the lattice to form an H-bonded one-dimensional polymer. Similarly, the lattice water present in **4** serves to link the zinc phenylphosphinate molecules through hydrogen bonding in the form of a 1-D polymer. The reaction of the precursor complex $[Zn(bpy)_2(OAc)](ClO_4) \cdot H_2O$ with dpp-H, dppi-H, and ppi-H in methanol leads to the formation of zinc phosphate $[Zn(bpy)_2(dpp)]_2(ClO_4)_2 \cdot H_2O$ (**5**) and phosphinates $[Zn(bpy)_2(dppi)]_2(ClO_4)_2$ (**6**) and $[Zn(bpy)_2(ppi)]_2(ClO_4)_2$ (**7**), respectively. The molecular structures of **1–5** and **7** have been determined by single-crystal X-ray diffraction studies.

(© Wiley-VCH Verlag GmbH & Co. KGaA, 69451 Weinheim, Germany, 2008)

Introduction

Our recent investigations in metal phosphate chemistry have centered on the synthesis and structural characterization of a variety of transition-metal di-*tert*-butyl phosphate (M-dtbp) complexes with interesting architectures and properties.^[1–8] Although our original interest in this area was in using di-*tert*-butyl phosphate complexes of transition metals as precursors for the preparation of metal phosphate materials due to the high thermal instability of these complexes, our latter investigations have shown that these complexes are useful model compounds for metal-catalyzed phosphate ester hydrolysis reactions.^[8] For example, the simple binary M-dtbp complexes of the type $[M(dtbp)_2]_n$ ($M = Mn, Co, Cu, Zn, Cd$) serve as excellent precursors for the preparation of respective fine-particle metal phosphate

materials $[M(PO_3)_2]$ at fairly low temperatures.^[2,3] Use of ancillary ligands such as 2,2'-bipyridine and 1,10-phenanthroline breaks the polymeric complexes down to lower oligomers and monomeric complexes due to chelation around the metal atom.^[2,8] Many of these compounds have been found to be useful model compounds for phosphate ester hydrolysis reactions.^[8]

Zinc phosphates have been focused upon in recent years both in light of the use of Zn^{II} ions in metal-promoted phosphate ester hydrolysis reactions,^[9] and open-framework metal phosphates, which show rich structural diversity.^[10–12] The isolation of zinc phosphate based molecular sieves in 1991^[10a] has impelled research on the synthesis and characterization of newer zinc phosphates and phosphonates. Stucky and co-workers have recently reported the first open-framework zinc phosphonate containing 24-ring channels.^[10d] Other zinc phosphates and phosphonates with one-, two-, and three-dimensional structures have also been reported.^[10–12] In contrast to metal phosphates and phosphonates possessing extended structures, their molecular analogues, at oligonuclear scale, have been receiving attention only in the last decade.^[13–17] These limited studies already suggest that the structures of the molecular metal phosphates and phosphonates are dependent on the type of

[a] Department of Chemistry, Indian Institute of Technology – Bombay, Powai, Mumbai 400076, India
Fax: +91-22-2572-3480
E-mail: rmv@chem.iitb.ac.in

[b] Department of Inorganic and Physical Chemistry, Indian Institute of Science, Bangalore 560012, India

[c] Department of Chemistry, Howard University, Washington, DC 20059, USA

metal precursor used, the substituents on the phosphorus atom, as well as the nature of any co-ligands employed for additional stabilization. It has been shown by Roesky et al. that the reaction of diethylzinc with *tert*-butylphosphonic acid in different stoichiometric ratios leads to the isolation of dodecanuclear, hexanuclear, and tetranuclear molecular phosphonate clusters $[\{Zn_2(THF)_2(ZnEt)_6Zn_4(\mu_4-O)(tBuPO_3)_8\}]$,^[14a] $[\{(ZnEt)_3[Zn(THF)]_3\}\{tBuPO_3\}_4\{\mu_3-OEt\}]$, and $[\{(ZnMe)_4(THF)_2\}\{tBuPO_3\}_2]$.^[14b] Reaction of zinc acetate (instead of $ZnMe_2$) with *tert*-butylphosphonic acid in the presence of 2-aminopyridine results in the isolation of cubane-like zinc phosphonate clusters which are arranged in the lattice as a 3-dimensional supramolecular framework with the aid of noncovalent interactions.^[13]

Among the zinc phosphates, the reaction of diethylzinc with di-*tert*-butyl phosphate (dtbp-H) yields a one-dimensional polymer $[Zn(dtbp)_2]_n$,^[16a,16b] while the same ligand reacts with zinc acetate and produces an oxido-bridged tetranuclear cluster $[Zn_4(\mu_4-O)(dtbp)_6]$.^[2] Using a monoorgano phosphate in the place of alkylphosphonic acid, we have shown that it is possible to assemble cubane-like $Zn_4O_{12}P_4$ polyhedral molecules and arrange them in 1-D, 2-D, and 3-

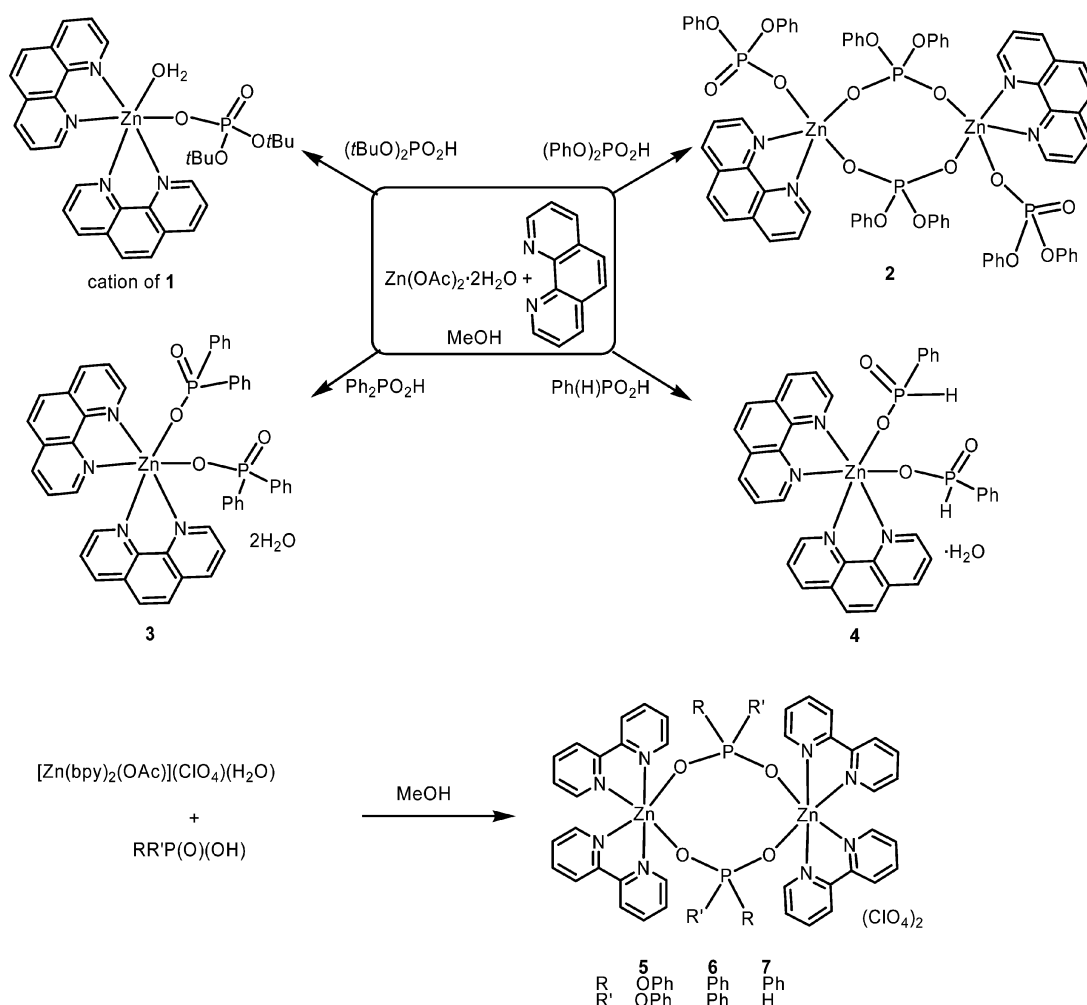
D supramolecular assemblies using noncovalent interactions.^[18]

In the present study, in order to explore the role of co-ligands, we have investigated the reaction of Zn^{II} salts or suitable zinc precursors with a series of phosphate esters and phosphinic acids in the presence of strongly chelating bidentate ligands 2,2'-bipyridine and 1,10-phenanthroline and isolated a variety of monomeric and dimeric zinc phosphates.

Results and Discussion

Syntheses

Zinc acetate was used as the starting material along with phosphate diesters and phosphinic acids to synthesize the new zinc complexes. The synthesis of zinc phosphates and phosphinates, $[Zn(phen)_2(dtbp)(OH_2)](dtbp)(MeOH)(MeCOOH)(H_2O)_3$ (**1**), $[\{Zn(phen)(dpp)\}_2\{\mu_2-dpp\}_2]$ (**2**), $[Zn(phen)_2(dppi)_2]\cdot 2H_2O$ (**3**), and $[Zn(phen)_2(ppi)_2]\cdot H_2O$ (**4**), has been achieved using a similar synthetic procedure, by treating 1 equiv. of zinc acetate dihydrate with 2 equiv.



Scheme 1. Synthesis of zinc phosphates and phosphinates **1**–**7**.

of the corresponding phosphate ester or phosphinic acid in the presence of 2 equiv. of 1,10-phenanthroline in methanol (Scheme 1).

In order to introduce more than one 2,2'-bipyridine on each zinc atom in the resultant phosphate, a zinc precursor with a noncoordinating anion, $[\text{Zn}(\text{bpy})_2(\text{OAc})](\text{ClO}_4) \cdot \text{H}_2\text{O}$, was chosen as the starting material. Thus, the reaction of $[\text{Zn}(\text{bpy})_2(\text{OAc})](\text{ClO}_4) \cdot \text{H}_2\text{O}$ with dpp-H, dppl-H, and ppi-H in methanol leads to the formation of zinc phosphate $[\text{Zn}(\text{bpy})_2(\text{dpp})]_2(\text{ClO}_4)_2 \cdot \text{H}_2\text{O}$ (**5**) and phosphinates $[\text{Zn}(\text{bpy})_2(\text{dppl})]_2(\text{ClO}_4)_2$ (**6**) and $[\text{Zn}(\text{bpy})_2(\text{ppi})]_2(\text{ClO}_4)_2$ (**7**), respectively (Scheme 1). The products have been obtained in good yields (>80%) in analytically pure form and characterized by means of IR, ^1H and ^{31}P NMR, UV/Vis absorption and emission spectroscopy. All compounds are air-stable and soluble in common organic solvents such as methanol, ethanol, tetrahydrofuran, dichloromethane, chloroform, and toluene.

Although the reactive part of the ligand which binds the metal atom in all the compounds is the same $-\text{P}(\text{O})(\text{OH})$ group, it is interesting to note that a different type of product is obtained from each of the reactions shown in Scheme 1. This is presumably due to the bulkiness of the phosphinate or phosphate ligand used as well as the electronic factors associated with the substituent on the phosphorus atom. In the case of zinc phosphinates **3** and **4** (dppl and ppi), the metal ion accommodates two phen ligands and two monodentate phosphinate ligands within the coordination sphere and achieves an octahedral geometry. In the cases of the zinc phosphates **1** and **2** (formed by dtbp and dpp), there is only one phosphate ligand bound to the metal atom in a monodentate fashion. While the second phosphate ligand is outside the coordination sphere of the metal atom in **1**, the second phosphate anion in **2** acts as a bridging ligand between two zinc ions to result in a dimeric complex. The presence of two bridging dpp ligands and one monodentate terminal dpp ligand around the metal atom leaves room only for one phen ligand, and hence the zinc ion in **2** is only five-coordinate, whereas the zinc ion in **1**, **3**, and **4** has an octahedral environment (see below for a full structure description). However, the introduction of noncoordinating ClO_4^- anions provides enough room for neutral ligands, and hence two 2,2'-bipyridine ligands coordinate around the metal atom in the dimeric complexes **5**–**7**, along with the two phosphate ligands that symmetrically bridge the two metal ions.

Spectral Characterization

The infrared spectra of compounds **1**–**7** show the characteristic vibrations expected for these molecules (Figure 1). The IR spectra for compounds **1**, **3**, **5**, and **4** show an absorption around 3400 cm^{-1} due to the presence of water (indicating that both coordinated and lattice water molecules are hydrogen-bonded). Absence of this peak in the infrared spectra of **2** and **7** indicates absence of water molecules either in the metal coordination sphere or in the lattice. The infrared peaks at 3066 and 2976 cm^{-1} for **1**, 3067 and

3046 cm^{-1} for **2**, 3113 and 3073 cm^{-1} for **5**, 3068 and 3049 cm^{-1} for **3**, 3049 and 2990 cm^{-1} for **4**, and 3068 and 3041 cm^{-1} for **7** are due to aromatic C–H vibrations. Additionally, the aliphatic C–H vibrations occur at 2931 cm^{-1} for the *tert*-butyl groups in **1**. The absorption in the infrared spectra of **4** and **7** at 2288 cm^{-1} and 2322 cm^{-1} , respectively, correspond to the P–H vibrations of the phenyl phosphinate moiety (Figure 1).

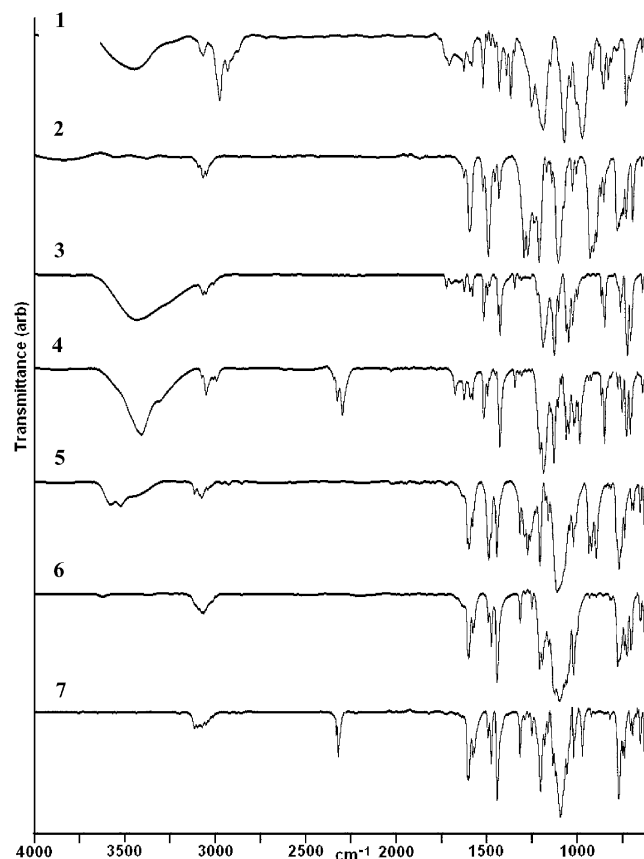


Figure 1. IR spectra of compounds **1**–**7** as KBr diluted discs.

The UV/Vis spectra of compounds **1**–**7** show a single absorption maximum in the range 292 – 309 nm , presumably originating from the aromatic substituents on the phosphorus atom as well as the 1,10-phenanthroline or 2,2'-bipyridine moiety. The fluorescence spectra of **1**–**7** are almost identical, and the emission maxima lie between 328 and 440 nm as shown in Figure 2. The fluorescence of the perchlorate complexes **5**–**7** was found to be much weaker than the neutral complexes **2**–**4** suggesting that the presence of the spherical ClO_4^- anion decreases the fluorescence quantum yield considerably. The singlet emission for compounds **1**–**4** has been found to show a single exponential decay. The fluorescence lifetimes of the complexes **1**–**4** were in the order of a few nanoseconds.

All the new zinc phosphates and phosphinates yielded a ^1H NMR spectral pattern which is consistent with their structure and constitution. For example, the ^1H NMR spectrum of $[\text{Zn}(\text{phen})_2(\text{dtbp})(\text{OH})](\text{dtbp})(\text{MeOH})(\text{MeCOOH})(\text{H}_2\text{O})_3$ (**1**) in CDCl_3 shows the presence of res-

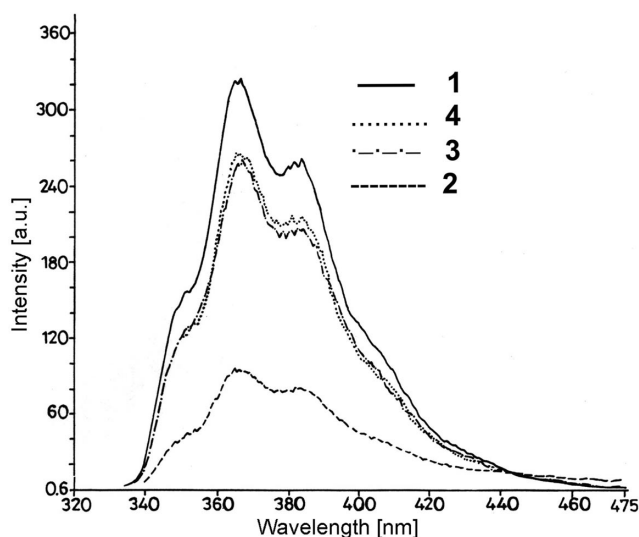


Figure 2. Fluorescence spectra for compounds **1–4** in CH₃OH.

onances at $\delta = 7.79, 7.93, 8.43$, and 9.22 ppm in a 1:1:1:1 ratio, which can be assigned to the protons of the 1,10-phenanthroline. The resonance appearing at $\delta = 2.02$ and 3.62 ppm can be assigned to the coordinated and the uncoordinated water molecules, respectively. The CH₃ protons of the *tert*-butoxy groups resonate as a singlet at $\delta = 1.25$ ppm. The ¹H NMR spectrum of compound **5** as a representative example is shown in Figure 3.

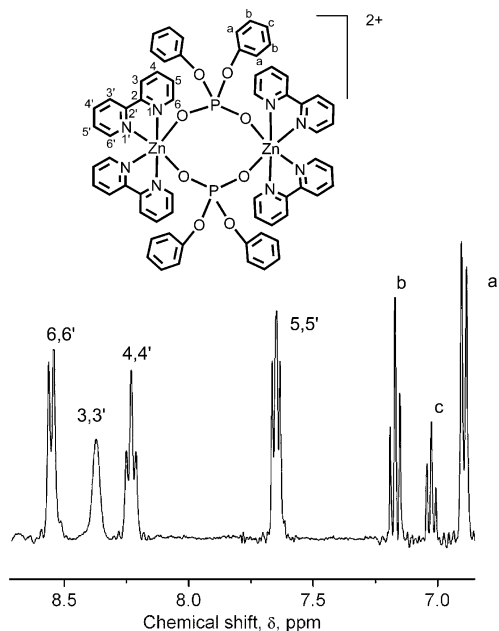


Figure 3. ¹H NMR spectrum of [Zn(bpy)₂(dpp)]₂(ClO₄)₂·H₂O (**5**) in CD₃OD.

The ³¹P NMR spectra of all the new phosphates show a single resonance indicating a symmetrical structure for the dinuclear complexes. The resonance observed for compounds **1–7** are schematically shown in Figure 4. While the resonance of diphenyl phosphinate and phenyl phosphinate complexes appears downfield, the phosphate complexes res-

onate upfield. It is surprising to note that compound **1** gives only a single ³¹P resonance at $\delta = -7.0$ ppm in spite of the presence of coordinated and uncoordinated dtbp ligands. This observation suggests the possibility of a different solution structure for this complex.

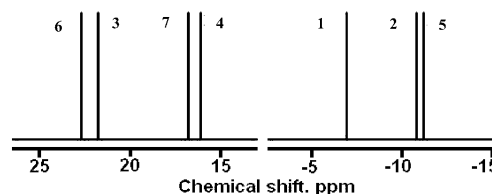


Figure 4. Schematic representation of the ³¹P NMR spectra of **1–7**.

Thermal Analysis

The TGA trace of **1** shows transitions starting from 35 °C caused by the loss of lattice water and solvent molecules (Figure 5). These transitions continue until ca. 200 °C where the organic part of the molecule of **1** is eliminated. Compound **2** shows the loss of phenyl groups when heated until 400 °C. For **3**, the TGA, when carried out under nitrogen shows transitions corresponding to loss of two water molecules, two phen molecules, and phenyl groups. The TGA of **4** shows a transition until 160 °C, caused by loss of one water molecule corresponding to a weight loss of 2.5%, followed by the loss of two phen molecules until 600 °C. Above 600 °C, the TGA traces of all the compounds show weight reductions presumably caused by the removal of P₂O₅. The powder X-ray diffraction pattern of the residues obtained after the thermolysis showed the presence of both Zn(PO₃)₂ and ZnP₂O₇ in varying proportions.

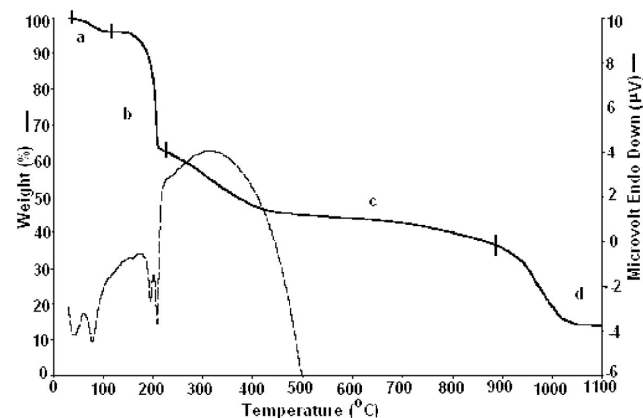


Figure 5. TGA/DTA trace of **1** [a = removal of H₂O, CH₃OH, CH₃COOH; b = removal of (CH₃)₂C=CH₂; c = removal of phen; d = removal of H₂O, P₂O₅].

Structure of 1

In order to ascertain the solid-state structures of the new zinc phosphates, a single-crystal X-ray diffraction study was

Table 1. Structural comparison of compounds 1–7.

Compound	av. Zn–O [Å]	av. Zn–N [Å]	Anion ^[a]	Nuclearity	Deviation from mean plane ^[b] [Å] Zn	P
1	2.025(5)	2.174(7)	dtbp	mononuclear	–	–
2	1.999(1)	2.145(1)	–	dinuclear	0.430	0.026
3	2.017(3)	2.195(3)	–	mononuclear	–	–
4	2.036(2)	2.204(2)	–	mononuclear	–	–
5	2.066(2)	2.167(2)	ClO ₄	dinuclear	0.006	0.243
7	2.070(4)	2.171(5)	ClO ₄	dinuclear	0.023	0.399

[a] Noncoordinating. [b] Plane passing through Zn–O–P–O–Zn–O–P–O atoms in cyclic phosphates.

carried out for most of the new compounds. In the case of compound 6, suitable single crystals could not be obtained. Selected structural data for the new compounds are compared in Table 1.

Single crystals of 1, suitable for X-ray diffraction studies, were obtained from a toluene/CH₂Cl₂ mixture (1:1) by slow evaporation of the solvent over a period of 2 d. The central Zn²⁺ ion in 1 is in an octahedral coordination environment. The coordination sphere consists of two phen moieties that are *cis* to each other, one dtbp ligand, and one water molecule (Figure 6). Charge balance is attained by the presence of one dtbp anion in the lattice. The asymmetric part of the unit cell in 1 consists of two [Zn(dtbp)(phen)₂(OH₂)] cations and two dtbp anions linked through extensive hydrogen bonding with three water molecules, one methanol molecule, and one acetic acid molecule. The high thermal parameters of the lattice dtbp as well as the solvent molecules gives rise to somewhat high residual electron density as well as high *R* factors. The core structure of 1 depicting the coordination environment around the zinc atoms is shown in Figure 6. Successive attempts to eliminate lattice

solvent molecules by repeated evacuation of a sample of 1 followed by crystallization from a variety of solvents yielded single crystals of the same composition. Low-temperature X-ray data measurement also did not improve the quality of the data. The observed bond lengths for Zn–O and Zn–N linkages and associated bond angles are, however, comparable to the other zinc phosphate described below. Because of the presence of two chelating 1,10-phen ligands, the *cis* and *trans* octahedral angles deviate considerably from the ideal values (Figure 6).

Structure of 2

Single crystals for the X-ray measurement of [{Zn(phen)(dpp)}₂{μ₂-dpp}₂] (2) were obtained by crystallization of the sample from a THF solution at room temperature after 2 d of slow evaporation of the solvent. The compound crystallizes in the monoclinic *P*2₁/*n* space group. The molecule has a dimeric structure, with a center of symmetry, where two zinc atoms are linked to each other by two diphenyl phosphate ligands as shown in Figure 7. The central zinc atom in 2 is five-coordinate. Each metal ion is surrounded by the nitrogen atoms of 1,10-phenanthroline [Zn–N(1) 2.191(1) and Zn–N(2) 2.099(1) Å], two bridging diphenyl phosphate oxygen atoms [Zn–O(21) 2.044(1) and Zn–O(22) 1.990(1) Å], and one terminal diphenyl phosphate oxygen atom [Zn–O(11) 1.963(1) Å]. The geometry around the Zn²⁺ ion could not be termed either regular trigonal-bipyramidal or square-pyramidal. The ten angles observed around the central Zn²⁺ ions, however, are closer to a distorted trigonal-bipyramidal geometry than a square-pyramidal geometry. For example, the angles observed fall into three ranges: 109.2–131.0° (basal angles), 77.0–96.7° (*cis* angles), and 164.1° (*trans* angle). The presence of only one *trans* angle (closer to the value of 180°) rules out the possibility of square-pyramidal geometry. In the distorted trigonal-bipyramidal geometry around the zinc ion in 2, it could be assumed that one bridging phosphate oxygen atom, one terminal phosphate oxygen atom, and one pyridyl nitrogen atom occupy the basal position while the second phenanthroline nitrogen atom and third phosphate group (bridging) occupy the axial site. This also explains the longer distance observed for the Zn–N(1) bond compared to the Zn–N(2) bond of the phen ligand and longer Zn–O(21)#1 bond compared to the Zn–O(11) and Zn–

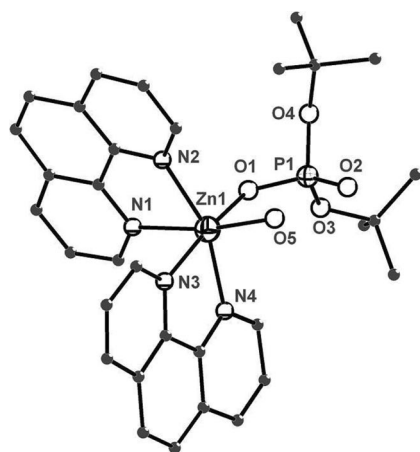


Figure 6. Molecular structure of one of the cations of [Zn(phen)₂(dtbp)(H₂O)₂(dtbp)₂-(CH₃COOH)(CH₃OH)(H₂O)₃] (1). Selected bond lengths [Å] and angles [°]: Zn(1)–O(1) 2.025(5), Zn(1)–O(5) 2.061(6), Zn(1)–N(4) 2.129(7), Zn(1)–N(2) 2.143(6), Zn(1)–N(3) 2.196(6), Zn(1)–N(1) 2.227(7); O(1)–Zn(1)–O(5) 89.2(2), O(1)–Zn(1)–N(4) 96.4(2), O(5)–Zn(1)–N(4) 98.4(3), O(1)–Zn(1)–N(2) 97.7(2), O(5)–Zn(1)–N(2) 96.0(3), N(4)–Zn(1)–N(2) 159.9(3), O(1)–Zn(1)–N(3) 172.5(2), O(5)–Zn(1)–N(3) 93.5(2), N(4)–Zn(1)–N(3) 76.3(3), N(2)–Zn(1)–N(3) 89.0(3), O(1)–Zn(1)–N(1) 88.3(2), O(5)–Zn(1)–N(1) 171.0(2), N(4)–Zn(1)–N(1) 90.5(2), N(2)–Zn(1)–N(1) 75.8(3), N(3)–Zn(1)–N(1) 90.1(2).

O(22) bonds. The central $\text{Zn}_2\text{P}_2\text{O}_4$ core as a whole exists in a pseudo- C_4 crown conformation, and resembles the single four-ring (S4R) SBUs of the zeolite materials.^[19]

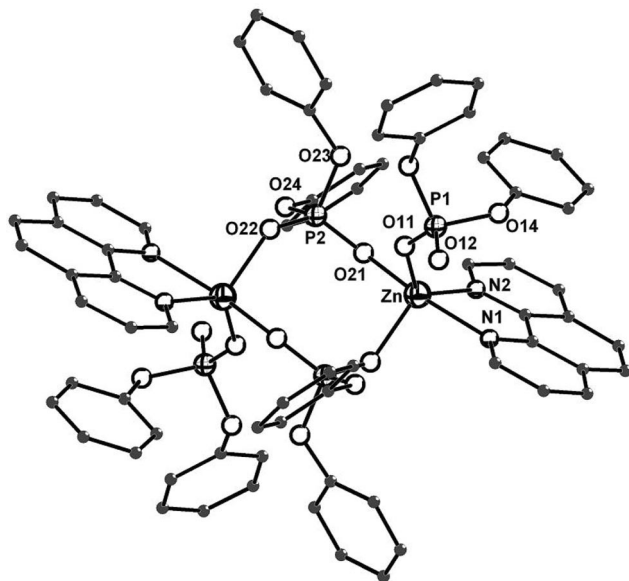


Figure 7. Molecular structure of $[\{\text{Zn}(\text{phen})(\text{dpp})\}_2\{\mu_2\text{-dpp}\}_2]$ (**2**). Selected bond lengths [Å] and angles [°]: Zn–O(11) 1.963(1), Zn–O(22) 1.990(1), Zn–O(21)#1 2.044(1), Zn–N(2) 2.099(1), Zn–N(1) 2.191(1), P(1)–O(12) 1.459(1), P(1)–O(11) 1.491(1); O(11)–Zn–O(22) 109.23(5), O(11)–Zn–O(21)#1 94.94(5), O(22)–Zn–O(21)#1 94.96(5), O(11)–Zn–N(2) 130.99(5), O(22)–Zn–N(2) 119.35(5), O(21)#1–Zn–N(2) 87.29(5), O(11)–Zn–N(1) 96.70(5), O(22)–Zn–N(1) 91.29(5), O(21)–Zn–N(1) 164.19(5), N(1)–Zn–N(2) 76.99(5). Symmetry transformations used to generate equivalent atoms: #1: $-x, 2-y, z$.

Structure of 3

Compound $[\text{Zn}(\text{phen})_2(\text{dppi})_2]\cdot 2\text{H}_2\text{O}$ (**3**) was crystallized from THF at room temperature. Colorless single crystals of **3**, obtained after 2 d by slow evaporation of the solvent,

crystallize in the monoclinic $P2_1/n$ space group. The Zn^{2+} ion in $[\text{Zn}(\text{phen})_2(\text{dppi})_2]\cdot 2\text{H}_2\text{O}$ is octahedrally coordinated by two phen and two dppi ligands (Figure 8). The two dppi anions bind the metal atom in a unidentate fashion and are *cis* to each other [O(1)–Zn(1)–O(3) 94.3(1)°]. The major difference between the structure of **2** and **3** is that, in the latter compound the phosphinate ligand exclusively binds to the metal ion in a terminal monodentate fashion. The P=O functionalities are not involved in coordination to the metal atom. These uncoordinated phosphoryl oxygen atoms of the diphenyl phosphinate ligands form intermolecular

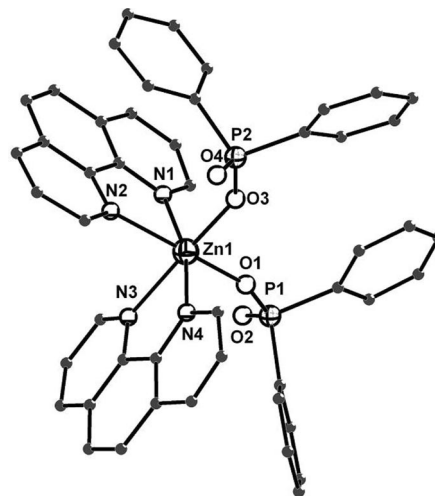


Figure 8. Molecular structure of $[\text{Zn}(\text{phen})_2(\text{dppi})_2]\cdot 2\text{H}_2\text{O}$ (**3**). Selected bond lengths [Å] and angles [°]: Zn(1)–O(1) 2.003(3), Zn(1)–O(3) 2.030(3), Zn(1)–N(4) 2.136(3), Zn(1)–N(1) 2.145(3), Zn(1)–N(2) 2.243(3), Zn(1)–N(3) 2.256(3), P(1)–O(2) 1.482(3), P(1)–O(1) 1.501(3), P(2)–O(4) 1.494(3), P(2)–O(3) 1.508(3) Å; O(1)–Zn(1)–O(3) 94.3(1), O(1)–Zn(1)–N(4) 96.1(1), O(3)–Zn(1)–N(4) 95.4(1), O(1)–Zn(1)–N(1) 93.8(1), O(3)–Zn(1)–N(1) 94.8(1), N(4)–Zn(1)–N(1) 165.2(1), O(1)–Zn(1)–N(2) 167.7(1), O(3)–Zn(1)–N(2) 92.4(1), N(4)–Zn(1)–N(2) 93.6(1), N(1)–Zn(1)–N(2) 75.3(1), O(1)–Zn(1)–N(3) 89.8(1), O(3)–Zn(1)–N(3) 170.3(1), N(4)–Zn(1)–N(3) 75.4(1), N(1)–Zn(1)–N(3) 93.7(1), N(2)–Zn(1)–N(3) 85.2(1).

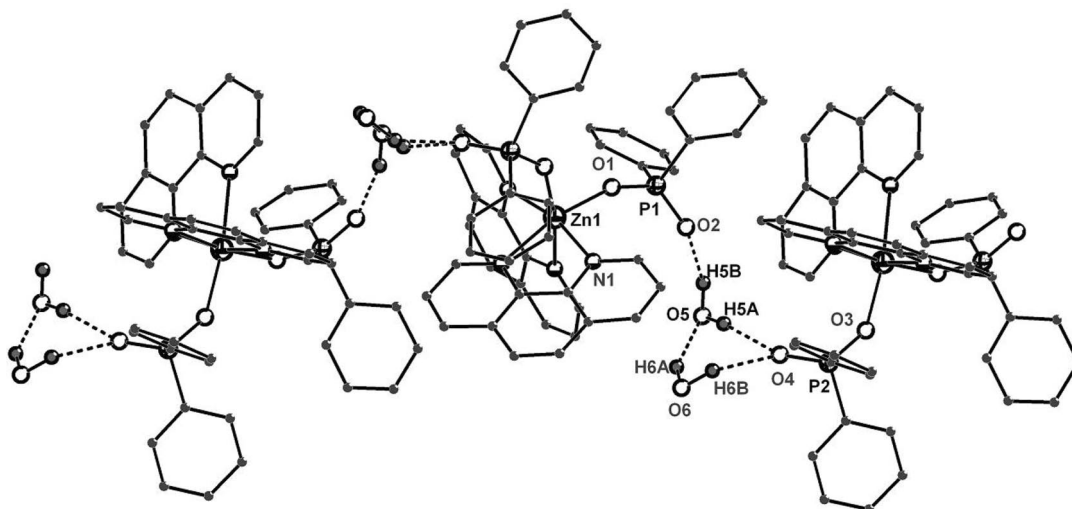


Figure 9. Packing diagram of the molecules of **3** in the solid state along the *a*-axis showing the formation of lattice water dimer linkers.

hydrogen bonds with the two water molecules present in the lattice (per asymmetric part). These water molecules also hydrogen-bond with each other. The $[\text{Zn}(\text{dppi})_2(\text{phen})_2]$ units are interconnected through water dimer molecules with the aid of hydrogen bonding between water hydrogen atoms and the phosphoryl oxygen atoms, and this results in the formation of a chain as shown in Figure 9.

It is of interest to have a closer look at the water dimers sandwiched in the lattice of **3** between the phosphinate moieties (Figure 10) in light of the attention the $(\text{H}_2\text{O})_2$ dimer has received in recent years.^[20,21] Although the structure of the water dimer was characterized by molecular beam experiments as early as 1977,^[22] the existence of such dimeric units in organic^[23] and inorganic^[24,25] host lattices has been studied only recently. The formation of the water dimer in **3** represents a case of capture of the water dimer between free P=O groups in the lattice. These two water molecules have only one hydrogen bond between them ($\text{O6} \cdots \text{H6A} \cdots \text{O5}$), as has also been determined for the water dimer by both gas-phase studies^[22] and solid-state crystal diffraction in organic and inorganic lattices.^[23–25] In addition to the solitary hydrogen bond between the two water molecules, the water dimer is involved in three additional hydrogen bonds to the P=O oxygen atoms in the neighborhood. For example, both the hydrogen atoms of O5 are involved in $\text{P}=\text{O} \cdots \text{H}-\text{O}$ interaction with two different phosphinate moieties on either

side. Similarly, the H6B atom on O6 forms a hydrogen bond with O4 of the phosphinate ligand on one side. This is a slightly different situation compared to the earlier examples of water dimer found in inorganic frameworks,^[24,25] where the dimer is normally held by the metal-coordinated water molecule rather than an $\text{M}=\text{O}$ or an $\text{E}=\text{O}$ acceptor.

Structure of **4**

Compound $[\text{Zn}(\text{phen})_2(\text{ppi})_2] \cdot \text{H}_2\text{O}$ (**4**) was crystallized from acetonitrile at room temperature by slow evaporation of the solvent over 2 d. Colorless single crystals of **4** crystallize in the orthorhombic $P2_1ab$ space group. The structure of **4** is very similar to that of **3**. The Zn^{2+} ion in **4** is octahedrally coordinated by two chelating phen ligands and two terminal ppi ligands (Figure 11). The two ppi anions bind to the metal atom in a unidentate fashion and are *cis* to each other [$\text{O}(21)-\text{Zn}-\text{O}(11)$ $92.11(7)^\circ$]. The P=O functionalities are not involved in coordination to the metal atom. Thus, the replacement of one of the phenyl substituents on the phosphorus atom by a hydrogen atom does not bring about any change in the structure of the metal phosphate formed. The uncoordinated phosphoryl oxygen atoms of the phenyl phosphinate ligands form intermolecular hydrogen bonds with the lattice water molecule (Figure 12) to form a 1-D polymer.

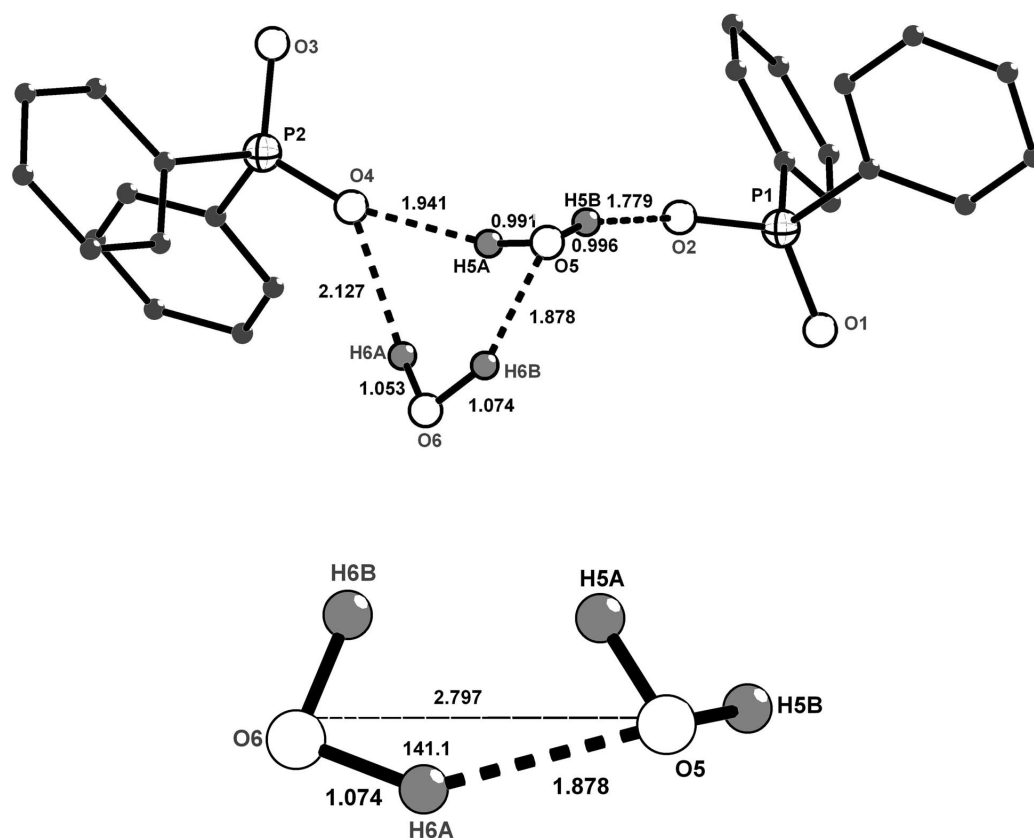


Figure 10. Structure of the water dimer found in the crystal lattice of **3** and the associated bond lengths and angles.

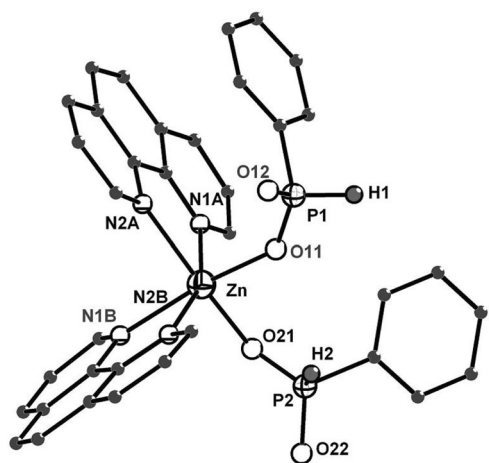


Figure 11. Molecular structure of $[\text{Zn}(\text{phen})_2(\text{ppi})_2](\text{H}_2\text{O})$ (**4**). Selected bond lengths [Å] and angles [°]: Zn–O(21) 2.032(2), Zn–O(11) 2.040(2), Zn–N(1A) 2.143(2), Zn–N(2B) 2.156(2), Zn–N(1B) 2.236(2), Zn–N(2A) 2.279(2), P(1)–O(12) 1.477(2), P(1)–O(11) 1.504(2), P(2)–O(22) 1.488(2), P(2)–O(21) 1.506(2), O(1W)–H(1W1) 0.81(1), O(1W)–H(1W2) 0.83(2) Å; O(21)–Zn–O(11) 92.11(7), O(21)–Zn–N(1A) 93.90(7), O(11)–Zn–N(1A) 98.13(7), O(21)–Zn–N(2B) 101.60(7), O(11)–Zn–N(2B) 95.09(8), N(1A)–Zn–N(2B) 159.21(7), O(21)–Zn–N(1B) 86.02(7), O(11)–Zn–N(1B) 170.27(7), N(1A)–Zn–N(1B) 91.53(7), N(2B)–Zn–N(1B) 75.98(8), O(21)–Zn–N(2A) 169.02(7), O(11)–Zn–N(2A) 91.50(7), N(1A)–Zn–N(2A) 75.32(7), N(2B)–Zn–N(2A) 88.40(7), N(1B)–Zn–N(2A) 92.10(7), O(12)–P(1)–O(11) 118.46(11).

Structure of 5

Compound $[\text{Zn}(\text{bpy})_2(\text{dpp})]_2(\text{ClO}_4)_2 \cdot \text{H}_2\text{O}$ (**5**) was crystallized from methanol at room temperature. Colorless single crystals of $[\text{Zn}(\text{bpy})_2(\text{dpp})]_2(\text{ClO}_4)_2 \cdot \text{H}_2\text{O}$ were obtained at room temperature by slow evaporation of the solvent. The compound crystallizes in the monoclinic $C2/c$ space group. As in the case of compound **2**, compound **5** is also made up of a $\text{Zn}_2\text{P}_2\text{O}_4$ central eight-membered ring that resembles the S4R SBU of zeolites. The major difference between **2** and **5** is the absence of terminal monodentate

dpp ligands on the zinc centers, which have been replaced by the noncoordinated perchlorate ligands. As a result, the zinc ions are able to accommodate an additional 1,10-phen ligand. Thus, the dpp ligands in **5** act as bidentate bridging ligands, where two dpp ligands bridge two Zn atoms $[\text{Zn}(1)–\text{O}(1)$ 2.082(2) Å; $\text{Zn}(1)–\text{O}(2)$ 2.049(2) Å] and form a dimer. Each Zn atom in the dimeric structure is coordinated by two bpy ligands resulting in an octahedral geometry around the metal ions (Figure 13). As expected, the (Zn)O–P bonds [av. 1.469(2) Å] are shorter than the (C)O–P bonds

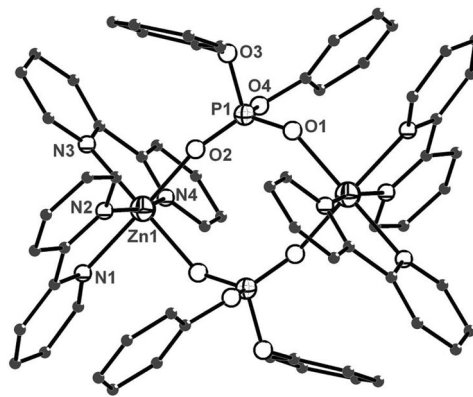


Figure 13. Molecular structure of the $[\text{Zn}(\text{bpy})_2(\text{dpp})]_2^{2+}$ cation in **5**. Selected bond lengths [Å] and angles [°]: Zn(1)–O(1) 2.082(2), Zn(1)–O(2) 2.049(2), Zn(1)–N(1) 2.162(2), Zn(1)–N(2) 2.144(2), Zn(1)–N(3) 2.226(2), Zn(1)–N(4) 2.134(2), P(1)–O(2)#1 1.468(2), P(1)–O(1) 1.469(2), P(1)–O(4) 1.583(2), P(1)–O(3) 1.604(2); N(4)–Zn(1)–N(2) 167.68(9), O(2)–Zn(1)–N(1) 166.48(8), O(1)–Zn(1)–N(3) 166.85(9), O(2)–Zn(1)–O(1) 95.09(8), O(2)–Zn(1)–N(4) 92.60(9), O(1)–Zn(1)–N(4) 92.37(9), O(2)–Zn(1)–N(2) 90.47(8), O(1)–Zn(1)–N(2) 99.24(8), O(1)–Zn(1)–N(1) 84.55(8), N(4)–Zn(1)–N(1) 100.92(8), N(2)–Zn(1)–N(1) 76.28(8), O(2)–Zn(1)–N(3) 89.36(9), N(4)–Zn(1)–N(3) 75.0(1), N(2)–Zn(1)–N(3) 93.08(9), N(1)–Zn(1)–N(3) 93.98(9), O(2)#1–P(1)–O(1) 118.9(1), O(2)#1–P(1)–O(4) 108.0(1), O(1)–P(1)–O(4) 111.3(1), O(2)#1–P(1)–O(3) 108.6(1), O(1)–P(1)–O(3) 108.9(1), O(4)–P(1)–O(3) 99.4(1). Symmetry transformations used to generate equivalent atoms: #1: $3/2 - x$, $1/2 - y$, $-z$.

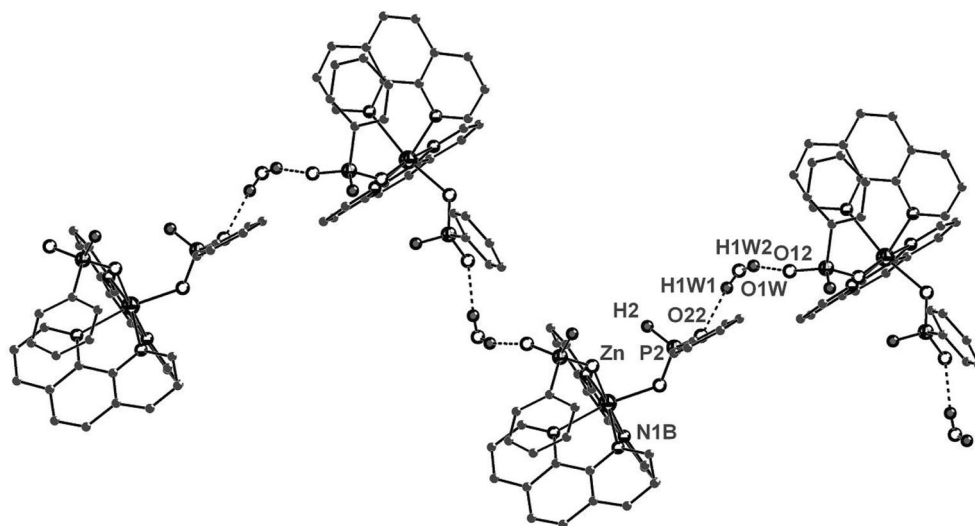


Figure 12. Packing of the molecules of **4** in the solid state showing the formation of lattice water monomer linkers along the c -axis.

[av. 1.594(2) Å], and the (Zn)O–P–O(Zn) bond angle [O(2) #1–P(1)–O(1) 118.9(1)°] is wider than the (C)O–P–O(C) bond angle [O(4)–P(1)–O(3) 99.4(1)°]. The central eight-membered ring exists in a crown conformation.

Structure of 7

Compound $[\text{Zn}(\text{bpy})_2(\text{ppi})]_2(\text{ClO}_4)_2$ (**7**) crystallizes from methanol at room temperature. Although the compound crystallizes in the triclinic $P\bar{1}$ space group, the observed molecular structure of **7** is very similar to that observed for **5** described above (Figure 14), with the only difference being the substituents on the phosphorus atom of the phosphinate ligand.

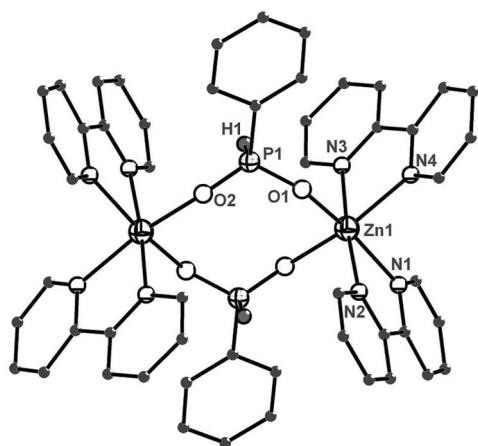


Figure 14. Molecular structure of the $[\text{Zn}(\text{bpy})_2(\text{ppi})]_2^{2+}$ cation in **7**. Selected bond lengths [Å] and angles [°]: Zn(1)–O(1) 2.062(4), Zn(1)–O(2)#1 2.077(4), Zn(1)–N(2) 2.160(5), Zn(1)–N(3) 2.165(5), Zn(1)–N(4) 2.169(5), Zn(1)–N(1) 2.189(4), P(1)–O(2) 1.493(4), P(1)–O(1) 1.496(4), O(1)–Zn(1)–O(2)#1 97.3(2), O(1)–Zn(1)–N(2) 88.8(2), O(2)#1–Zn(1)–N(2) 94.20(2), O(1)–Zn(1)–N(3) 94.8(2), (2) #1–Zn(1)–N(3) 88.5(2), N(2)–Zn(1)–N(3) 175.2(2), O(1)–Zn(1)–N(4) 86.7(2), O(2)#1–Zn(1)–N(4) 164.2(2), N(2)–Zn(1)–N(4) 101.2(2), N(3)–Zn(1)–N(4) 75.9(2), O(1)–Zn(1)–N(1) 163.9(2), O(2) #1–Zn(1)–N(1) 85.9(2), N(2)–Zn(1)–N(1) 75.2(2), N(3)–Zn(1)–N(1) 101.1(2), N(4)–Zn(1)–N(1) 94.6(2), O(2)–P(1)–O(1) 117.2(2). Symmetry transformations used to generate equivalent atoms: #1: 2 – x, –y, 1 – z.

Conclusions

The structural diversity in molecular zinc phosphates and phosphinates resulting from both electronic and steric factors has been investigated. Different types of products were obtained in each reaction depending on the steric bulk and the electronic factors associated with the substituent on the phosphorus atom and the nature of the metal precursors. When the noncoordinating perchlorate containing complex $[\text{Zn}(\text{bpy})_2(\text{OAc})](\text{ClO}_4) \cdot \text{H}_2\text{O}$ was used as the starting material, the product obtained in each case was a dimer (compounds **5**–**7**). When zinc acetate was used as the starting material, the products formed were found to be monomers if two phen ligands are attached to the metal atom. If only one phen ligand is attached to the zinc atom, then the

product formed is a dimer. In all cases, where two chelating ligands are bound to the zinc atom, the coordination geometry of the zinc atom is octahedral. When only one chelating ligand is attached to the metal atom, the coordination geometry around the zinc atom is distorted trigonal-bipyramidal. All the neutral zinc complexes prepared in this study were found to be highly fluorescent with excited life-times of the order of a few nanoseconds. The cationic complexes were, however, found to be only weakly emitting from the excited singlet state. Finally, in complexes where the phosphinate ligand coordinates to the metal atom in a monodentate terminal fashion with P=O groups on the ligand, water molecules were found to be captured due to the formation of strong $\text{P}=\text{O} \cdots \text{H}-\text{O}$ hydrogen bonds. In the case of complex **3**, this leads to the observation of an interesting water dimer.

Experimental Section

Instruments and Methods: Elemental analyses were performed with a Carlo Erba (Italy) Model 1106 Elemental Analyzer at IIT, Bombay. Infrared spectra were recorded with a Perkin-Elmer FT-IR spectrometer as KBr diluted discs. ^1H and ^{31}P NMR spectra were recorded with Bruker AS 300 and Varian 400S spectrometers using Me_4Si (external) as a reference for ^1H NMR and 85% H_3PO_4 (external) as a reference for ^{31}P NMR spectral measurements. Thermal analyses were carried out with a Perkin-Elmer thermal analysis system. For generating organic free metal phosphates, the samples were placed in an Al_2O_3 boat and kept inside a furnace. Samples were allowed to calcine inside the furnace at a constant temperature over 12 h in air and then cooled to room temperature gradually.

Solvents and Starting Materials: Commercial-grade solvents were purified by employing conventional procedures and distilled prior to use.^[26] Commercially available starting materials such as $\text{Zn}(\text{OAc})_2 \cdot 2\text{H}_2\text{O}$ (Ortanal, Italy), 2,2'-bipyridine (Lancaster), 1,10-phenanthroline monohydrate (s.d. Fine-Chem), diphenyl phosphate (Lancaster), diphenylphosphinic acid (Lancaster), phenylphosphinic acid (Lancaster), and NaClO_4 (Aldrich) were used as received. $[\text{Zn}(\text{OAc})(\text{bpy})_2]\text{ClO}_4 \cdot \text{H}_2\text{O}$ ^[27] and $(\text{tBuO})_2\text{PO}_2\text{H}$ ^[28] were synthesized as described previously in the literature.

Synthesis of 1: $[\text{Zn}(\text{OAc})_2 \cdot 2\text{H}_2\text{O}]$ (219 mg, 1 mmol) was dissolved in methanol (20 mL), and phen (396 mg, 2 mmol) was added. To the resultant solution, dtbp-H (420 mg, 2 mmol) was added, and the mixture was stirred. The solvent was removed from the resultant mixture in vacuo, and the solid obtained was dissolved in toluene/ CH_2Cl_2 and left to crystallize at room temperature. Colorless crystals obtained after 2 d were found to be suitable for X-ray diffraction studies. Yield: 0.75 g (80%). M.p. 135–137 °C. $\text{C}_{83}\text{H}_{122}\text{N}_8\text{O}_{24}\text{P}_4\text{Zn}_2$ (1870.6): calcd. C 53.29, H 6.57, N 5.99; found C 53.3, H 6.5, N 6.0. IR (KBr): $\tilde{\nu}$ = 3434 (m), 3066 (m), 2976 (m), 2931 (w), 1705 (m), 1519 (m), 1430 (m), 1136 (m), 1252 (m), 1183 (s), 1070 (vs), 969 (vs), 852 (m), 825 (s), 730 (m), 720 (m) cm^{-1} . UV/Vis (CH_3OH): λ (ε) = 294 (21627 $\text{cm}^{-1} \text{M}^{-1}$) nm. Fluorescence (λ_{ex} = 300 nm, CH_3OH): λ = 365, 381 nm. ^1H NMR (CD_3OD , 400 MHz): δ = 1.2 (s, 18 H, CH_3 , *t*Bu), 2.0 (s, 3 H, CH_3COOH), 3.6 (br., 9 H, H_2O , CH_3OH), 7.79, 7.93, 8.43, 9.22 (4 m, 16 H, phen CH) ppm. ^{31}P NMR (CD_3OD , 162 MHz): δ = –7.0 ppm. TGA: Temp. range (weight loss) = 30–65 (2.9%), 65–150 (3.6%), 150–214 (31.9%), 214–800 (23.0%) °C. DSC: 43 (endo), 80 (endo), 196 (endo), 209 (endo) °C.

Synthesis of 2: $[\text{Zn}(\text{OAc})_2 \cdot 2\text{H}_2\text{O}]$ (219 mg, 1 mmol) was dissolved in methanol (20 mL). To this solution, dpp-H (500 mg, 2 mmol) was added, after which the reaction mixture became turbid. To the resultant solution, phen (396 mg, 2 mmol) was added and the mixture stirred. The solution became clear. The solvent was removed from the resultant mixture in vacuo, and the greasy solid obtained was dissolved in THF by heating at 70 °C and leaving for crystallization at room temperature. Colorless crystals obtained after 2 d were found suitable for X-ray diffraction studies. Yield: 0.66 g (89%). M.p. 189–191 °C. $\text{C}_{72}\text{H}_{56}\text{N}_4\text{O}_{16}\text{P}_4\text{Zn}_2$ (1487.9): calcd. C 58.12, H 3.79, N 3.77; found C 57.2, H 3.8, N 3.7. IR (KBr): $\tilde{\nu}$ = 3067 (m), 3046 (m), 1593 (m), 1490 (m), 1430 (w), 1292 (s), 1267 (s), 1209 (vs), 1102 (vs), 927 (vs), 850 (m), 766 (s), 727 (m), 690 (m) cm^{-1} . UV/Vis (CH_3OH): λ (ϵ) = 296 (8599 $\text{cm}^{-1}\text{M}^{-1}$) nm. Fluorescence (λ_{ex} = 300 nm, CH_3OH): λ = 366, 382 nm. ^1H NMR (CD_3OD , 300 MHz): δ = 6.8–7.2 (m, 40 H, phenyl CH), 7.85, 8.13, 8.72, 8.91 (4 m, 16 H, phen CH) ppm. ^{31}P NMR (CD_3OD , 121 MHz): δ = –11.2 ppm. TGA: Temp. range (weight loss) = 30–404 (41.0%, – 2 C_6H_5) °C. DSC: 192 (endo) °C.

Synthesis of 3: $[\text{Zn}(\text{OAc})_2 \cdot 2\text{H}_2\text{O}]$ (219 mg, 1 mmol) was dissolved in methanol (20 mL). To this solution, dppi-H (436 mg, 2 mmol) was added, after which the reaction mixture became turbid. To the resultant solution, phen (396 mg, 2 mmol) was added and the mixture stirred. The solvent was removed from the resultant mixture in vacuo, and the greasy solid obtained was dissolved in THF by heating at 70 °C. The resultant solution was left for crystallization at room temperature. Colorless crystals obtained after 2 d, were found suitable for X-ray diffraction studies. Yield: 0.75 g (84%). M.p. 174–176 °C. $\text{C}_{48}\text{H}_{40}\text{N}_4\text{O}_6\text{P}_2\text{Zn}$ (896.2): calcd. C 64.33, H 4.50, N 6.25; found C 63.1, H 4.6, N 6.2. IR (KBr): $\tilde{\nu}$ = 3443 (vs), 3340 (vs), 3068 (m), 3049 (m), 1689 (s), 1621 (s), 1578 (s), 1423 (s), 1188 (vs), 1124 (vs), 1046 (vs), 1023 (vs), 998 (s), 845 (s), 756 (s), 721 (s), 702 (s), 556 (s) cm^{-1} . UV/Vis (CH_3OH): λ (ϵ) = 302 (2595 $\text{cm}^{-1}\text{M}^{-1}$) nm. Fluorescence (λ_{ex} = 300 nm, CH_3OH): λ = 366, 380 nm. ^1H NMR (CD_3OD , 300 MHz): δ = 7.01, 7.13, 7.36 (3 m, 20 H, phenyl CH), 8.08, 8.28, 8.63, 8.67 (4 m, 16 H, phen CH) ppm. ^{31}P NMR (CD_3OD , 121 MHz): δ = 21.4 ppm. TGA: Temp. range (weight loss) = 30–180 (4.0%, – 2 H_2O), 180–456 (40.0%, – 2 phen), 500–800 (26.0%, C_6H_5) °C. DSC: 153 (endo), 192 (endo), 254 (endo), 558 (endo) °C.

Synthesis of 4: $[\text{Zn}(\text{OAc})_2 \cdot 2\text{H}_2\text{O}]$ (219 mg, 1 mmol) was dissolved in methanol (20 mL). To this solution, ppi-H (284 mg, 2 mmol) was added, after which the reaction mixture became turbid. To the resultant solution, phen (396 mg, 2 mmol) was added and the mixture stirred. Then the solution became clear. The solvent was removed from the resultant mixture in vacuo, and the greasy compound obtained was dissolved in acetonitrile/THF (1:1). This solution was left for crystallization at room temperature. Colorless crystals obtained after 2 d were found suitable for X-ray diffraction studies. Yield: 0.61 g (84%). M.p. 162–164 °C. $\text{C}_{36}\text{H}_{30}\text{N}_4\text{O}_5\text{P}_2\text{Zn}$ (726.0): calcd. C 59.56, H 4.17, N 7.72; found C 59.1, H 4.3, N 7.2. IR (KBr): $\tilde{\nu}$ = 3407 (br.), 3307 (br.), 3049 (m), 2990 (w), 2288 (s), 1673 (m), 1623 (m), 1585 (m), 1513 (m), 1426 (s), 1204 (s), 1190 (vs), 1140 (s), 1015 (s), 984 (s), 860 (m), 736 (m), 544 (m) cm^{-1} . UV/Vis (CH_3OH): λ (ϵ) = 300 (5309 $\text{cm}^{-1}\text{M}^{-1}$) nm. Fluorescence (λ_{ex} = 300 nm, CH_3OH): λ = 366, 381 nm. ^1H NMR (CD_3OD , 400 MHz): δ = 6.85, 7.07, 7.23 (3 m, 10 H, phenyl CH), 7.91, 8.00, 8.15, 8.75 (4 m, 16 H, phen CH) ppm. ^{31}P NMR (CD_3OD , 121 MHz): δ = 16.3 ppm. TGA: Temp. range (weight loss) = 30–160 (2.5%, – H_2O), 160–600 (50.3%, – 2 phen) °C. DSC: 166 (endo) °C.

Synthesis of 5: $[\text{Zn}(\text{OAc})(\text{bpy})_2](\text{ClO}_4) \cdot \text{H}_2\text{O}$ (554 mg, 1 mmol) was dissolved in methanol (80 mL), and dpp-H (250 mg, 1 mmol) was

added. The resulting solution was stirred for 1 h and filtered. The product crystallized from the filtrate at room temperature, and X-ray quality crystals were obtained. Yield: 0.65 g (88%). M.p. 245–248 °C. $\text{C}_{64}\text{H}_{56}\text{Cl}_2\text{N}_8\text{O}_{17}\text{P}_2\text{Zn}_2$ (1472.8): calcd. C 52.19, H 3.83, N 7.61; found C 52.4, H 3.2, N 7.6. IR (KBr): $\tilde{\nu}$ = 3572 (w), 3522 (w), 3113 (w), 3073 (w), 1606 (m), 1596 (m), 1578 (w), 1488 (m), 1443 (m), 1316 (w), 1292 (w), 1273 (m), 1260 (w), 1204 (s), 1161 (w), 1111 (vs), 1042 (w), 1020 (vs), 936 (m), 920 (w), 895 (m), 767 (s), 756 (m), 737 (m), 699 (w), 688 (w), 652 (w), 622 (m), 527 (w), 513 (w) cm^{-1} . ^1H NMR (CD_3OD , 400 MHz): δ = 6.88, 7.02, 7.15 (3 m, 20 H, phenyl CH), 7.65, 8.23, 8.37, 8.56 (4 m, 32 H, bpy CH) ppm. ^{31}P NMR (CD_3OD , 121 MHz): δ = –11.5 ppm. UV/Vis (CH_3OH): λ (ϵ) = 309 (17697 $\text{cm}^{-1}\text{M}^{-1}$) nm. Fluorescence (λ_{ex} = 309 nm, CH_3OH): λ = 329 nm. TGA: Temp. range (weight loss) = 200–269 (8.8%), 270–449 (53.6%), 450–792 (10.6%), 793–1015 (7.1%) °C. DSC: 196 (endo); 256 (endo); 350 (exo) °C.

Synthesis of 6: $[\text{Zn}(\text{OAc})(\text{bpy})_2](\text{ClO}_4)(\text{H}_2\text{O})$ (360 mg, 0.6 mmol) was dissolved in methanol (60 mL). To this solution, $\text{Ph}_2\text{PO}_2\text{H}$ (327 mg, 1.5 mmol) was added, and the mixture was stirred for 30 min and then filtered. The filtrate was kept at room temperature for crystallization. X-ray diffraction quality crystals were obtained from the solution. Yield: 0.5 g (86.4%). M.p. >260 °C. $\text{C}_{32}\text{H}_{26}\text{ClN}_4\text{O}_6\text{PZn}$ (694.4): calcd. C 55.35, H 3.77, N 8.07; found C 55.1, H 3.6, N 8.1. IR (KBr): $\tilde{\nu}$ = 3063 (w), 1597 (m), 1578 (w), 1568 (w), 1491 (w), 1474 (m), 1442 (s), 1313 (m), 1249 (w), 1206 (m), 1191 (m), 1158 (w), 1122 (s), 1097 (vs), 1070 (s), 1057 (s), 1018 (m), 776 (m), 737 (w), 723 (m), 702 (m), 651 (w), 623 (m) cm^{-1} . ^1H NMR (CD_3OD , 400 MHz): δ = 7.18, 7.29, 7.40 (3 m, 20 H, phenyl CH), 7.64, 8.20, 8.49 (3 m, 32 H, bpy CH) ppm. ^{31}P NMR (CD_3OD , 121 MHz): δ = 22.5 ppm. UV/Vis (CH_3OH): λ (ϵ) = 294 (32267 $\text{cm}^{-1}\text{M}^{-1}$) nm. TGA: Temp. range (weight loss) = 178–264 (9.2%, – 2 O_2), 265–418 (45.0%, – 2 bpy), 419–538 (11.1%, – Ph), 539–925 (11.1%, – Ph) °C. DSC: 251 (endo), 301 (endo), 369 (exo) °C.

Synthesis of 7: $[\text{Zn}(\text{OAc})(\text{bpy})_2](\text{ClO}_4)(\text{H}_2\text{O})$ (360 mg, 0.6 mmol) was dissolved in methanol (60 mL), and ppi-H (213 mg, 1.5 mmol) was added. The resulting solution was stirred for 1 h and filtered. The filtrate was left at room temperature for crystallization. X-ray diffraction quality crystals were obtained from this solution after a few days. Yield: 0.5 g (81%). M.p. 250–252 °C. $\text{C}_{26}\text{H}_{22}\text{ClN}_4\text{O}_6\text{PZn}$ (618.3): calcd. C 50.51, H 3.59, N 9.06; found C 50.5, H 3.3, N 9.0. IR (KBr): $\tilde{\nu}$ = 3437 (br.), 3113 (w), 3071 (w), 3050 (w), 2924 (w), 2854 (m), 2347 (w), 1604 (m), 1577 (w), 1567 (w), 1492 (w), 1475 (m), 1441 (s), 1315 (m), 1250 (w), 1201 (m), 1180 (w), 1161 (w), 1134 (m), 1120 (m), 1090 (vs), 1054 (m), 1019 (m), 971 (m), 771 (s), 747 (w), 738 (w), 704 (w), 692 (m), 651 (w), 624 (m) cm^{-1} . ^1H NMR (DMSO , 400 MHz): δ = 6.82, 6.98, 7.20 (3 m, 10 H, phenyl CH), 7.40, 7.60, 8.20, 8.80 (4 m, 32 H, bpy CH) ppm. ^{31}P NMR (CD_3OD , 121 MHz): δ = 16.8 ppm. UV/Vis (CH_3OH): λ (ϵ) = 306 (31205 $\text{cm}^{-1}\text{M}^{-1}$) nm. Fluorescence (λ_{ex} = 306 nm, CH_3OH): λ = 328 nm. TGA: Temp. range (weight loss) = 180–296 (10.4%), 297–515 (50.4%), 516–969 (12.7%) °C. DSC: 296 (exo); 354 (exo) °C.

X-ray Structure Determination of 1–5 and 7: Single crystals suitable for X-ray diffraction studies were obtained in each case directly from the reaction mixture at room temperature. Where necessary, the crystals were re-grown from appropriate solutions. X-ray diffraction data were obtained for compounds 1–5 and 7 either with a STOE-AED2 diffractometer, Oxford XCalibur system, or a Bruker AXS diffractometer. In each case, the data obtained up to 2θ = 50° were used for all the calculations. The structure solutions were achieved by using direct methods as implemented in SHELXS-97.^[29] The structures were refined by full least-squares methods

Table 2. Crystal data for 1–5 and 7.

	1	2	3	4	5	7
Identification code	mur42	rp187	mur32	rp236	rp509	rp513
Empirical formula	C ₈₃ H ₁₂₂ N ₈ O ₂₄ P ₄ Zn ₂	C ₃₆ H ₂₈ N ₂ O ₈ P ₂ Zn	C ₄₈ H ₄₀ N ₄ O ₆ P ₂ Zn	C ₃₆ H ₃₀ N ₄ O ₅ P ₂ Zn	C ₆₄ H ₅₄ Cl ₂ N ₈ O ₁₇ P ₂ Zn ₂	C ₂₆ H ₂₂ ClN ₄ O ₆ PZn
Formula mass	1870.51	743.91	896.15	725.95	1470.73	618.27
Temperature [K]	150(2)	293(2)	203(2)	293(2)	293(2)	293(2)
Wavelength [Å]	0.71073	0.71073	0.71073	0.71073	0.71073	0.71073
Crystal system	triclinic	monoclinic	monoclinic	orthorhombic	monoclinic	triclinic
Space group	<i>P</i> $\bar{1}$	<i>P</i> 2 ₁ / <i>n</i>	<i>P</i> 2 ₁ / <i>c</i>	<i>P</i> 2 ₁ <i>ab</i>	<i>C</i> 2/ <i>c</i>	<i>P</i> $\bar{1}$
<i>a</i> [Å]	10.905(2)	13.5432(8)	17.830(4)	18.0320(7)	27.326(8)	8.800(5)
<i>b</i> [Å]	16.315(3)	10.7558(7)	12.216(2)	9.8067(4)	14.220(4)	11.527(5)
<i>c</i> [Å]	26.928(5)	23.659(2)	19.166(4)	19.0176(7)	19.170(6)	14.458(5)
α [°]	79.73(3)					67.842(5)
β [°]	85.64(3)	100.660(1)	92.03(3)		116.228(4)	86.732(5)
γ [°]	84.38(3)					87.607(5)
<i>V</i> [Å ³]	4683(2)	3386.9(4)	4172(1)	3363.0(2)	6682(3)	1356(1)
<i>Z</i>	2	4	4	4	4	2
<i>D</i> (calcd.) [Mg/m ³]	1.326	1.459	1.427	1.434	1.462	1.515
Absorption coefficient [mm ^{−1}]	0.655	0.875	0.722	0.875	0.920	1.111
<i>F</i> (000)	1976	1528	1856	1496	3016	632
Crystal size [mm]	0.85 × 0.55 × 0.45	0.25 × 0.2 × 0.2	1.00 × 0.70 × 0.30	0.10 × 0.40 × 0.42	0.71 × 0.38 × 0.23	0.29 × 0.17 × 0.06
θ range [°]	3.64–21.20	1.90 to 29.40	3.50–25.02	2.26–28.28	1.81–28.02	1.52–28.36
Data/restraints/parameters	9970/0/1114	8619/0/442	7325/0/706	7343/4/449	8001/0/429	6408/0/440
Goodness-of-fit on <i>F</i> ²	1.037	1.025	1.058	0.998	1.023	1.009
<i>R</i> ₁ [<i>I</i> > 2 σ (<i>I</i>)]	0.0900	0.0312	0.0557	0.0291	0.0471	0.0823
<i>R</i> ₂ [<i>I</i> > 2 σ (<i>I</i>)]	0.2378	0.0796	0.1330	0.0663	0.1254	0.1721

using SHELXL-97.^[30] The hydrogen atoms, where possible, were identified from the difference maps and included in the calculations. All other hydrogen atoms were geometrically fixed and then refined using a riding model. The non-hydrogen atoms were treated anisotropically during the refinement. The hydrogen atoms were refined with isotopic thermal parameters. For all the compounds, the refinements converged to good *R* factors with no appreciable residual electronic densities. The crystal data and refinement details are given in Table 2. CCDC-669686 (1), -669687 (2), -669688 (3), -669689 (4), -669690 (5), and -669691 (7) contain the supplementary crystallographic data for this paper. These data can be obtained free of charge from The Cambridge Crystallographic Data Centre via www.ccdc.cam.ac.uk/data_request/cif.

Acknowledgments

This work was supported by the Department of Science and Technology, New Delhi, in the form of a Young Scientist (Fast Track) Project to M. G. W. and a Swarnajayanti Fellowship to R. M. We thank the Sophisticated Instrument Facility, Indian Institute of Technology – Bombay for analytical and spectroscopic data. R. P. and S. S. thank the Council of Scientific and Industrial Research for a research fellowship.

- [1] R. Murugavel, M. G. Walawalkar, M. Dan, H. W. Roesky, C. N. R. Rao, *Acc. Chem. Res.* **2004**, *37*, 763.
- [2] R. Murugavel, M. Sathiyendiran, M. G. Walawalkar, *Inorg. Chem.* **2001**, *40*, 427.
- [3] M. Sathiyendiran, R. Murugavel, *Inorg. Chem.* **2002**, *41*, 6404.
- [4] R. Murugavel, M. Sathiyendiran, R. Pothiraja, M. G. Walawalkar, T. Mallah, E. Riviere, *Inorg. Chem.* **2004**, *43*, 945.
- [5] R. Pothiraja, M. Sathiyendiran, R. J. Butcher, R. Murugavel, *Inorg. Chem.* **2004**, *43*, 7585.
- [6] R. Pothiraja, M. Sathiyendiran, R. J. Butcher, R. Murugavel, *Inorg. Chem.* **2005**, *44*, 6314.
- [7] R. Murugavel, M. Sathiyendiran, *Chem. Lett.* **2001**, *1*, 84.

- [8] R. Murugavel, M. Sathiyendiran, R. Pothiraja, R. J. Butcher, *Chem. Commun.* **2003**, 2546.
- [9] a) K. Weis, M. Rombach, M. Ruf, H. Vahrenkamp, *Eur. J. Inorg. Chem.* **1998**, 263; b) H. Brombacher, H. Vahrenkamp, *Inorg. Chem.* **2004**, *43*, 6050; c) J. A. Maldonado Calvo, H. Vahrenkamp, *Inorg. Chim. Acta* **2006**, *359*, 4079; d) M. M. Ibrahim, J. Seebacher, G. Steinfeld, H. Vahrenkamp, *Inorg. Chem.* **2005**, *44*, 8531; e) M. Ji, H. Vahrenkamp, *Eur. J. Inorg. Chem.* **2005**, 1398.
- [10] a) T. M. Nenoff, W. T. A. Harrison, T. E. Gier, G. D. Stucky, *J. Am. Chem. Soc.* **1991**, *113*, 378; b) T. E. Gier, G. D. Stucky, *Nature* **1991**, *349*, 508; c) P. Feng, X. Bu, G. D. Stucky, *Angew. Chem. Int. Ed. Engl.* **1995**, *34*, 1745; d) J. Zhu, X. Bu, P. Feng, G. D. Stucky, *J. Am. Chem. Soc.* **2000**, *122*, 11563.
- [11] a) S. Neeraj, S. Natarajan, C. N. R. Rao, *J. Solid State Chem.* **2000**, *150*, 417; b) S. Neeraj, S. Natarajan, C. N. R. Rao, *Angew. Chem. Int. Ed.* **1999**, *38*, 3480; c) S. Neeraj, S. Natarajan, C. N. R. Rao, *J. Chem. Soc., Dalton Trans.* **2000**, 2499; d) S. Neeraj, C. N. R. Rao, A. K. Cheetham, *J. Mater. Chem.* **2004**, *14*, 814.
- [12] a) S. Mandal, S. Natarajan, *Inorg. Chim. Acta* **2004**, *357*, 1437; b) Y. Wang, J. Yu, M. Guo, R. Xu, *Angew. Chem. Int. Ed.* **2003**, *42*, 4089; c) Y. Song, J. Yu, G. Li, Y. Li, Y. Wang, R. Xu, *Chem. Commun.* **2002**, 1720; d) A. Choudhury, S. Neeraj, S. Natarajan, C. N. R. Rao, *J. Mater. Chem.* **2002**, *12*, 1044.
- [13] R. Murugavel, S. Shanmugan, *Chem. Commun.* **2007**, 1257.
- [14] a) Y. Yang, J. Pinkas, M. Noltemeyer, H.-G. Schmidt, H. W. Roesky, *Angew. Chem. Int. Ed.* **1999**, *38*, 664; b) G. Anantharaman, V. Chandrasekhar, M. G. Walawalkar, H. W. Roesky, D. Vidovic, J. Magull, M. Noltemeyer, *Dalton Trans.* **2004**, 1271.
- [15] a) V. Chandrasekhar, S. Kingsley, B. Rhatigan, M. K. Lam, A. L. Rheingold, *Inorg. Chem.* **2002**, *41*, 1030; b) V. Chandrasekhar, P. Sasikumar, R. Boomishankar, G. Anantharaman, *Inorg. Chem.* **2006**, *45*, 3344.
- [16] a) C. G. Lugmair, T. D. Tilley, A. L. Rheingold, *Chem. Mater.* **1997**, *9*, 339; b) C. G. Lugmair, T. D. Tilley, *Inorg. Chem.* **1998**, *37*, 1821.
- [17] a) R. Murugavel, S. Kuppuswamy, *Angew. Chem. Int. Ed.* **2006**, *45*, 7022; b) R. Murugavel, S. Shanmugan, S. Kuppuswamy, *Eur. J. Inorg. Chem.*, DOI: 10.1002/eqic.200701032.

- [18] R. Murugavel, S. Kuppuswamy, R. Boomishankar, A. Steiner, *Angew. Chem. Int. Ed.* **2006**, *45*, 5536.
- [19] Ch. Baerlocher, W. M. Meier, D. H. Olson, *Atlas of Zeolite Framework Types*, 5th ed., Elsevier, Amsterdam, **2001**.
- [20] a) D. P. Schofield, J. R. Lane, H. G. Kjaergaard, *J. Phys. Chem. A* **2007**, *111*, 567; b) S. Scheiner, *Ann. Rev. Phys. Chem.* **1994**, *45*, 23; c) N. Goldman, C. Leforestier, R. J. Saykally, *J. Phys. Chem. A* **2004**, *108*, 787; d) R. Ludwig, *Angew. Chem. Int. Ed.* **2001**, *40*, 1808.
- [21] J. A. Anderson, G. S. Tschumper, *J. Phys. Chem. A* **2006**, *110*, 7268.
- [22] a) T. R. Dyke, K. M. Mack, J. S. Muentner, *J. Chem. Phys.* **1977**, *66*, 498; b) J. A. Odutola, T. R. Dyke, *J. Chem. Phys.* **1980**, *72*, 5062; R. S. Fellers, C. Leforestier, L. B. Braly, M. G. Brown, R. J. Saykally, *Science* **1999**, *284*, 945.
- [23] D. K. Chand, P. K. Bharadwaj, *Inorg. Chem.* **1998**, *37*, 5050.
- [24] S. Manikumari, V. Shivaiah, S. K. Das, *Inorg. Chem.* **2002**, *41*, 6953 and references cited therein.
- [25] S. K. Ghosh, P. K. Bharadwaj, *Inorg. Chem.* **2003**, *42*, 8250.
- [26] a) D. D. Perrin, W. L. F. Armarego, *Purification of Laboratory Chemicals*, 3rd ed., Pergamon Press, Elmsford, NY, **1988**; b) *Vogel's Text Book of Practical Organic Chemistry*, 5th ed., Langman Group, Essex, Harlow, UK, **1989**.
- [27] X.-M. Chen, Z.-T. Xu, T. C. W. Mak, *Polyhedron* **1994**, *13*, 3329.
- [28] A. Zwierzak, M. Kluba, *Tetrahedron* **1971**, *27*, 3163.
- [29] G. M. Sheldrick, *SHELXS-97: Program for crystal structure solution*, University of Göttingen, Germany, **1997**.
- [30] G. M. Sheldrick, *SHELXL-97: Program for crystal structure refinement*, University of Göttingen, Germany, **1997**.

Received: October 2, 2007

Published Online: February 20, 2008